ERDC/EL SR-22-2

Environmental Laboratory

US Army Corps of Engineers®
Engineer Research and Development Center

Aquatic Nuisance Species Research Program

A Review of Empirical Algorithms for the Detection and Quantification of Harmful Algal Blooms Using Satellite-Borne Remote Sensing

Richard A. Johansen, Molly K. Reif, Christina L. Saltus, and Kaytee L. Pokrzywinski

June 2022

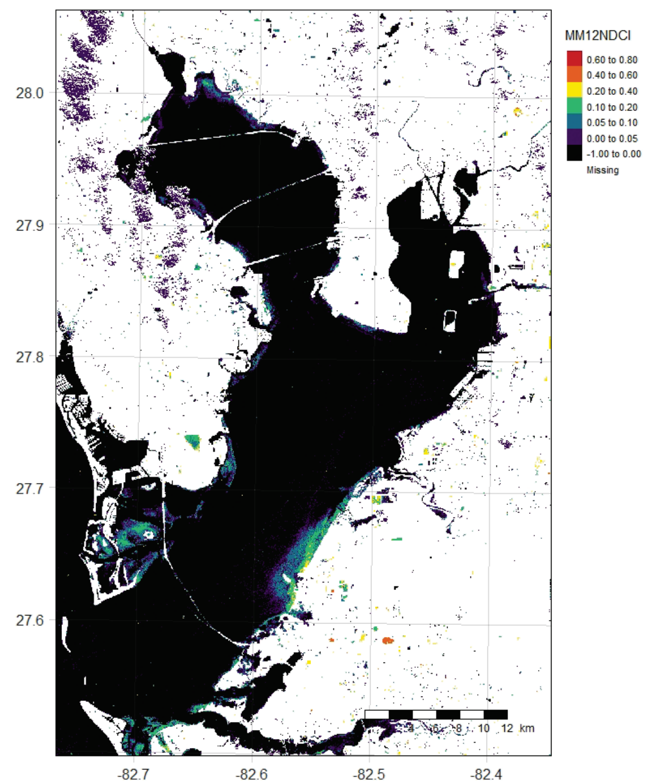

A Review of Empirical Algorithms for the Detection and Quantification of Harmful Algal Blooms Using Satellite-Borne Remote Sensing

Richard A. Johansen and Christina L. Saltus

Environmental Laboratory
U.S. Army Engineer Research and Development Center
3909 Halls Ferry Road
Vicksburg, MS 39180-6199

Molly K. Reif

Environmental Laboratory
U.S. Army Engineer Research and Development Center
Joint Airborne Lidar Bathymetry Technical Center of Expertise
7225 Stennis Airport Rd. Suite 100
Kiln, MS 39556

Kaytee Pokrzywinski

National Centers for Coastal Ocean Science
National Oceanic and Atmospheric Administration
101 Pivers Island Rd
Beaufort, NC 28516

Final report

Prepared for Aquatic Nuisance Species Research Program US Army Engineer Research and Development Center Environmental Laboratory Vicksburg, MS 39180-6199

Under Project 008284, “Comprehensive satellite-based algorithms for broadscale cyanoHAB detection and monitoring”
Funding Account Code U4377111
AMSCO Code 096 3123 495

Abstract

Harmful Algal Blooms (HABs) continue to be a global concern, especially since predicting bloom events including the intensity, extent, and geographic location, remain difficult. However, remote sensing platforms are useful tools for monitoring HABs across space and time. The main objective of this review was to explore the scientific literature to develop a near-comprehensive list of spectrally derived empirical algorithms for satellite imagers commonly utilized for the detection and quantification HABs and water quality indicators. This review identified the 29 WorldView-2 MSI algorithms, 25 Sentinel-2 MSI algorithms, 32 Landsat-8 OLI algorithms, 9 MODIS algorithms, and 64 MERIS/Sentinel-3 OLCI algorithms. This review also revealed most empirical-based algorithms fell into one of the following general formulas: two-band difference algorithm (2BDA), three-band difference algorithm (3BDA), normalized-difference chlorophyll index (NDCI), or the cyanobacterial index (CI). New empirical algorithm development appears to be constrained, at least in part, due to the limited number of HAB-associated spectral features detectable in currently operational imagers. However, these algorithms provide a foundation for future algorithm development as new sensors, technologies, and platforms emerge.

Contents

Figures and Tables

Figures

Tables

Preface

This study was conducted for the Aquatic Nuisance Species Research Program (ANSRP) under Project 008284, “Comprehensive satellite-based algorithms for broadscale cyanoHAB detection and monitoring.” The Acting Technical Monitor was Mr. Michael Greer.

The work was performed by the Environmental Systems Branch of the Ecosystem Evaluation and Engineering Division, US Army Engineer Research and Development Center, Environmental Laboratory (ERDC-EL). Technical reviews and discussions of this report were provided by Dr. Glenn Suir of the ERDC-EL and Mr. Sam Jackson of ERDC-EL.

At the time of publication, Mr. Mark R. Graves was the Chief of the Environmental Systems Branch; Mr. Mark D. Farr was Chief of Ecosystem Evaluation and Engineering Division; and Dr. Jennifer Seiter-Moser was the Technical Director for Environmental Engineering and Sciences. The Deputy Director of ERDC-EL was Dr. Jack E. Davis and the Director was Dr. Edmond J. Russo.

The Commander of ERDC was COL Teresa A. Schlosser and the Director was Dr. David W. Pittman.

1 Introduction

1.1 Background

The US Army Corps of Engineers (USACE) is the nation's largest federal provider of outdoor recreation, hosting over 370 million visitors a year at 4,300 recreation areas, centered around a network of over 400 lakes in 43 states. Over the past several decades, the US has experienced a notable increase in occurrence, intensity, and extent of Harmful Algal Blooms (HABs), which can cause adverse health impacts to humans and animals, as well as significant disruptions to local economies (Anderson et al. 2000; Linkov et al. 2009; USEPA 2012a, b). Thus, monitoring hundreds of at-risk inland lakes and reservoirs remains a critical function of the USACE. Unfortunately, monitoring these with traditional techniques is limited due to the cost- and labor-intensive nature of point-based sampling (Lunetta et al. 2015). In contrast, remote sensing-derived approaches can provide a cost-effective complement to detecting and quantifying HABs at a regional scale, which stands to improve situational awareness by helping to quickly identify and direct management actions to at-risk areas (Agha et al. 2012; Kutser et al. 2020; Matthews and Odermatt 2015; Mishra et al. 2017; Wynne et al. 2008).

HABs frequently occur in complex waterways, containing three or more independent optically active constituents, such as phytoplankton (chlorophylls), organic matter (CDOM), tripton, etc. As such, imaging satellites must be equipped with sensors that have appropriate spectral resolutions to not only detect these optically active constituents, but also distinguish between them. Fortunately, there are several satellite-based sensors capable of producing imagery for estimating key water quality parameters, such as chlorophyll *a* (chl-*a*), phycocyanin (PC), and turbidity. This is conducted by applying algorithms to important spectral features, such as the following: green reflectance (550 nm), phycocyanin absorption (620 nm), chlorophyll-a reflectance (665 nm - 680 nm), and cell backscattering (709 nm) (Davis et al. 2007; Lekki et al. 2019; Shen et al. 2012; Stumpf et al. 2016). In this context, algorithms are spectrally derived mathematical formulas that can be utilized to quantify water quality indicators. The lower spatial resolution satellite imagers like Envisat's MEdium Resolution Imaging Spectrometer (MERIS), Terra and Aqua's Moderate Resolution Imaging Spectroradiometer (MODIS), and

Sentinel-3's Ocean and Land Colour Instrument (OLCI), have spatial resolutions of 300 m, 250-1000 m, and 300 m, respectively (Table 1). All three of these imagers have been shown to be effective at detecting HABs and associated pigments in coastal marine environments as well as large fresh waterbodies, such as the Great Lakes (Augusto-Silva et al. 2014; Candiani et al. 2005; Carvalho et al. 2010; Clark et al. 2017; Coffer et al. 2020; Giardino et al. 2005; Gower et al. 2004; Hu et al. 2005; Urquahart and Schaeffer 2019). The spectral resolution of MERIS and OLCI can detect cyanoHABs because they are tuned to detect the cyanobacteria-specific pigment, phycocyanin, which has an absorption peak around 620 nm, and may help distinguish between cyanobacteria and other algal species. This is important in the US where most toxic HABs are dominated by the cyanobacteria, specifically *Microcystis* spp. However, these coarse spatial resolution sensors contain large instantaneous fields of view (IFOV), which are not suitable for smaller inland waterbodies that are likewise impacted by HABs.

In addition to MERIS/OCLI, there are a handful of satellite imagers with moderate to high spatial resolution but with lower spectral resolution, including Landsat-8's Operational Land Imager (L8-OLI), Sentinel-2 MultiSpectral Instrument (S2-MSI), and Worldview-2 MultiSpectral Instrument (WV2-MSI). These imagers have spatial resolution ranging from 1-60 m, making it possible to detect HABs and associated pigments in smaller inland waterbodies (Table 1). However, these imagers lack a narrow spectral band centered near 620 nm, making them incapable of detecting the 5-15 nm absorption feature caused by phycocyanin (Glazer et al. 1973). Another factor to be considered when utilizing a satellite to monitor water quality is revisit time. Revisit time is the time a satellite imager takes to re-image the same location, which depending on the orbit can vary from days to weeks. An emerging trend to improve revisit times without sacrificing spatial resolution is launching a constellation of identical imagers in complementary orbits.

In addition to satellite-borne imagers, there have been numerous successful airborne campaigns using high spatial and spectral resolution sensors that have provided excellent opportunities to develop and validate algorithms. Yet, these are typically ad-hoc or one-off events for a single waterbody to monitor a single bloom event. Generally, airborne imagery is effective for detailed mapping due to very high spatial and spectral resolutions, but not practical or cost-effective for routine or regional HAB monitoring. Thus, the appropriate choice for monitoring is dependent on the monitoring needs (e.g., species, toxins, etc.) and spatio-temporal scale of the waterbody. Regardless of sensor specifics or project scope, empirically based algorithms remain a valuable tool for monitoring HABs and estimating water quality related pigments.

Table 1. Satellite-borne sensors and technical specifications.

Imager	Center (nm)	Range (nm)	Bandwidth (nm)	GSD (m)
WV2-MSI				
b1	425	400–450	50	1.8
b2	480	450–510	60	1.8
b3	545	510–580	70	1.8
b4	605	585–625	40	1.8
b5	660	630–690	60	1.8
b6	725	705–745	40	1.8
b7	832.5	770–895	125	1.8
b8	950	860–1040	180	1.8
S2-MSI				
b1	443	433-453	20	20
b2	490.5	458–523	65	20
b3	560.5	543–578	35	20
b4	665	650–680	30	20
b5	705.5	698–713	15	20
b6	740.5	733–748	15	20
b7	783	773–793	20	20
b8	842.5	785–900	115	20
b9 (b8a)	865	855–875	20	20
L8-OLI				
b1	443	433-453	20	30
b2	480	450–510	60	30
b3	562.5	525–600	60	30
b4	655	630–680	30	30
b5	865	845–885	30	30
MODIS*				
b1	645	620–670	50	250
b2	858.5	841–876	35	250
B3	469	459-479	20	500

Imager	Center (nm)	Range (nm)	Bandwidth (nm)	GSD (m)
B4	555	545-565	20	500
B8	412.5	405-420	15	1000
B9	443	438-448	10	1000
B10	488	483-493	10	1000
B11	531	526-536	10	1000
B12	551	546-556	10	1000
B13	667	662-672	10	1000
B14	678	673-683	10	1000
B15	748	743-753	10	1000
B16	869.5	862-877	15	1000
B17	905	890-920	30	1000
B18	936	931-941	10	1000
B19	940	915-965	50	1000
MERIS				
b1	407	402–412	10	300
b2	443	438–448	10	300
b3	490	485–495	10	300
b4	510	505–515	10	300
b5	560	555–565	10	300
b6	620	615–625	10	300
b7	665	660–670	10	300
b8	681.5	678–685	7	300
b9	709	704–714	10	300
b10	753.5	750–757	7	300
b11	759.5	757–762	5	300
b12	779.5	772–787	15	300
b13	865	855–875	20	300
b14	885	880–890	10	300
b15	900	895–905	10	300
OLCI				
b01	400	392.5-407.5	15	300
b02	412.5	407.5-417.5	10	300
b03	442.5	437.5-447.5	10	300
b04	490	485-495	10	300
b05	510	505-515	10	300

Imager	Center (nm)	Range (nm)	Bandwidth (nm)	GSD (m)
b06	560	555-565	10	300
b07	620	615-625	10	300
b08	665	660-670	10	300
b09	673.75	670-677.5	7.5	300
b10	681.25	677.5-685	7.5	300
b11	708.75	703.75-713.75	10	300
b12	753.75	750-757.5	7.5	300
b13	761.25	760-762.5	2.5	300
b14	764.38	762.5-766.25	3.75	300
b15	767.5	766.25-768.75	2.5	300
b16	778.75	771.25-786.25	15	300
b17	865	855-875	20	300
b18	885	880-890	10	300
b19	900	895-905	10	300
b20	940	930-950	20	300
b21	1020	1000-1040	40	300

*MODIS bands greater than 1000 nm were not shown

Three algorithms commonly utilized for the estimation and monitoring of HABs are empirical, analytical, and semi-empirical. Empirical algorithms directly correlate remote sensing imagery to water quality constituents or HAB pigments using various statistical methods (Dekker 1993; Kallio et al. 2001; Mittenzwey et al. 1992; Simis et al. 2004). Analytical approaches quantify HABs by isolating a specific water quality constituent or HAB pigment from the remainder of the water's inherit optical properties (IOPs). Semi-empirical algorithms are a combination of empirical and analytical algorithms and optimize the model using one or more IOPs (Li 2017; Matthews 2011; Yan et al. 2018). Generally, analytical and semi-empirical algorithms tend to be more complex, requiring localized knowledge of a specific waterbody's IOPs. However, because empirical algorithms do not require localized knowledge, they present an opportunity to develop easy to deploy portable algorithms appropriate for regional monitoring applications.

Empirically based algorithms have been shown to successfully detect and quantify HAB related pigments such as, chlorophyll-a (Gitelson et al. 2009); cyanobacterial-specific pigment, phycocyanin (Ruiz-Verdu et al. 2008); and turbidity (Petus et al. 2010) but are known to be impacted by conditions under which the data were collected. For example, many algorithms were designed to be optimized for a particular study, limiting the algorithm's performance to a specific small geographic area, temporal or seasonal period, bio-physical parameter, or even constrained by the conditions in which the imagery was collected. Additionally, there are major challenges to the development of generalized spectrally based algorithms, including the lack of sufficient in-situ or in-vivo water quality data coupled with coincident remote sensing imagery across space and time, as well as the increasing complexities involved in algorithm development. Current data collection methods for detecting HABs vary widely in their spatial and temporal coverage. For example, field-based observations or water sampling provide detailed information but are limited to discrete locations across space and time. Stationary sondes can improve temporal coverage but are typically limited in spatial coverage and by the capacity and cost of probe-based water quality measurements. Ideally, algorithms should be evaluated using spatially dense water quality data coupled with near-coincident imagery. This is because HABs are extremely dynamic and respond rapidly to environmental changes which can vary on the order of hours to days (Dokulil and Teubner 2000; Hunter et al. 2008). This requires cost- and time-intensive field campaigns corresponding to same-day or near-same day satellite flyovers, which are routinely subject to disruptions due to cloud cover or inclement weather. Because of these challenges and data limitations, many previous studies were limited to localized algorithm development.

Notwithstanding, recent studies have demonstrated that many empirically based algorithms are effective and exhibit moderate to high levels of portability across space and time (Beck et al. 2016, 2017, 2018; Johansen et al. 2018). Dogliotti et al. (2015) describes a more valuable approach to algorithm development is focusing on generalizable algorithms, which can be applied across a set of defined parameters (i.e., "regional") or anywhere regardless of conditions (i.e., "global"). A list of generalizable algorithms would reduce technical barriers allowing for easier adoption of remote sensing methodologies for HAB monitoring at the local level.

1.2 Objective

Due to the rapidly evolving nature of water quality remote sensing, a literature review was required to compile historical and current research on empirical-based satellite-borne algorithms for the detection and estimation of cyanoHABs in inland waterways. The goal of this review is to compile these algorithms to further expand performance and portability testing of empirical algorithm-sensor combinations.

1.3 Approach

This report was conducted by compiling and reviewing a variety of peer-reviewed scientific articles, government reports, conference proceedings, and theses/dissertations to identify novel and modified satellite-based empirical algorithms for the estimation of three primary water quality parameters (chlorophyll *a*, phycocyanin, and turbidity). Articles focused on analytical and semi-analytical algorithms were excluded from this report due to the inability to implement these algorithms without localized knowledge of water characteristics. Although potentially useful, algorithms for marine algae or environments were also excluded to focus solely on freshwater environments.

2 Results

The following algorithms have been compiled from published research over the past three decades in waterbodies across the globe. Over the years, algorithms have been adapted and modified to be applicable to new optical sensors with varying spectral and spatial resolutions. To include these modified algorithms, multiple references were included where they have either been applied in another study or adapted to fit a new sensor. Note that algorithms have been documented to exhibit strong collinearity between multiple HAB-associated pigments or water quality indicators, especially when waterbodies are dominated by a single algal species or pigment. For simplicity, only the pigment or indicator of the original publication was listed (Tables 2 - 6).

Though water quality remote sensing has been around for decades and continues to become more integrated into monitoring programs, a standardized methodology has not been developed. For example, this review found significant variations in data collection strategies and analyses, image processing, and statistical approaches. Given these conflating factors, algorithm performances were deemed incomparable and thus omitted in the review.

2.1 WorldView-2 MSI

WorldView-2 imagery is commercially available through Maxar and available to the Department of Defense (DoD) as part of the National Geospatial Intelligence Agency's NextView License contract. WorldView-2 was launched in 2009 with a spatial resolution of 1.8 m, contains eight spectral bands (4 standard colors: red, blue, green, and near-IR; and 4 new colors: red edge, coastal, yellow, and near-IR2), and sun synchronous orbit with a revisit time of 1.1 days (DigitalGlobe 2009). This combination of high spatial and moderate spectral resolution is suitable for certain HAB detection and monitoring applications. A total of 29 WorldView-2 algorithms were identified and were fairly evenly distributed across the three water quality parameters, 10 chlorophyll *a* algorithms, 10 phycocyanin algorithms, and nine turbidity algorithms, respectively (Table 2). Although most of these were originally designed for other sensors, they were still found to be effective when original band centers were substituted for the nearest WorldView-2 band. Of particular interest for chl-*a* and PC, were the red-edge band (725 nm) and the red band

(660 nm). While turbidity algorithms often utilized a ratio of the NIR1 band (832 nm) to the blue band (480 nm) or green band (545 nm).

Table 2. WorldView-2 MSI empirically based algorithms.

Year	Parameter	Algorithm/Band Combination	Reference
1993	chl-a	$Rrs(600) - Rrs(648) - Rrs(625)$	Dekker 1993 Johansen et al. 2019
2007	chl-a	$\frac{Rrs(458) - Rrs(644)}{(Rrs529)}$	Kneubuhler et al. 2007 Johansen et al. 2019
2010	chl-a	$\frac{Rrs(857) - Rrs(644)}{Rrs(458) + Rrs(529)}$	Alawadi 2010 Johansen et al. 2019
2012	chl-a	$\frac{Rrs(709) - Rrs(665)}{Rrs(709) + Rrs(665)}$	Mishra and Mishra 2012 Wang et al. 2018 Johansen et al. 2019
2016	chl-a	$\frac{Rrs(725) - Rrs(660)}{Rrs(725) + Rrs(660)}$	Beck et al. 2016
2016	chl-a	$Rrs(545) - Rrs(660) + \left(Rrs(425) - Rrs(660)\right)$	Beck et al. 2016
2016	chl-a	$\frac{Rrs(725)}{Rrs(660)}$	Beck et al. 2016
2016	chl-a	$Rrs(660)^{-1} - Rrs(725)^{-1} * Rrs(832.5)$	Beck et al. 2016 Wang et al. 2018
2018	chl-a	$\frac{Rrs(724)}{Rrs(546)}$	Wang et al. 2018
2018	chl-a	$Rrs(724)$	Wang et al. 2018
2000	PC	$\frac{Rrs(650)}{Rrs(625)}$	Schalles and Yacobi 2000 Johansen et al. 2019
2004	PC	$Rrs(709) - Rrs(681) - \left(Rrs(753) - Rrs(681)\right) * \left(\frac{709 - 681}{753 + 681}\right)$	Gower et al. 2004 Johansen et al. 2019
2005	PC	$\frac{Rrs(709)}{Rrs(620)}$	Simis et al. 2005 Johansen et al. 2019
2008	PC	$-1 * Rrs(681) - Rrs(665) - (Rrs(709) - Rrs(665)) * \left(\frac{681 - 665}{709+665}\right)$	Wynne et al. 2008 Johansen et al. 2019

Year	Parameter	Algorithm/Band Combination	Reference
2009	PC	$\frac{Rrs(700)}{Rrs(600)}$	Mishra et al. 2009 Johansen et al. 2019
2009	PC	$\frac{Rrs(724)}{Rrs(609)}$	Mishra et al. 2009 Johansen et al. 2019
2008	PC	$(Rrs(615)^{-1} - Rrs(600)^{-1}) - Rrs(725)$	Hunter et al. 2008 Johansen et al. 2019
2012	PC	$\frac{Rrs(709)}{Rrs(600)}$	Mishra 2012 Johansen et al. 2019
2014	PC	$(Rrs(629)^{-1} - Rrs(659)^{-1}) * Rrs(724)$	Mishra and Mishra 2014 Johansen et al. 2019
2017	PC	$Rrs(725) - Rrs(605)$	Beck et al 2017
1980	Turb	$Rrs(658)$	Moore 1980 Johansen et al. 2019
1991	Turb	$\frac{Rrs(658)}{Rrs(458)}$	Lathrop et al. 1991 Johansen et al. 2019
1992	Turb	$Rrs(857)$	Schiebe et al. 1992 Johansen et al. 2019
2002	Turb	$\frac{Rrs(857)}{Rrs(658)}$	Doxaran et al. 2002 Johansen et al. 2019
2006	Turb	$\frac{Rrs(658)}{Rrs(558)}$	Bowers and Binding 2006 Johansen et al. 2019
2009	Turb	$\frac{Rrs(857)}{Rrs(558)}$	Chipman et al. 2009 Johansen et al. 2019
2009	Turb	$\frac{(Rrs(558) + Rrs(658)}{Rrs(458)}$	Frohn and Autrey 2009 Beck et al. 2018
2018	Turb	$\frac{(Rrs(558) + Rrs(658)}{Rrs(444)}$	Beck et al. 2018
2018	Turb	$\frac{Rrs(658)}{Rrs(444)}$	Beck et al. 2018

2.2 Sentinel-2 MSI

Launched in 2015 and 2017, the European Space Agency's (ESA) Copernicus is a constellation comprised of Sentinel-2A and Sentinel-2B l. Each sentinel-2 satellite contains multispectral imagers with 13 spectral bands with spatial resolutions varying from 10 m to 60 m (ESA 2015a). However, for analyses, the 10 m are down sampled to the coarser 20 m resolution so algorithm arithmetic is possible. The 60-m spectral bands are outside the usable range for HAB detection. Since the launch of Sentinel-2B in 2017, the typical revisit time has improved to roughly five days.

Sentinel-2's spatial resolution, weekly revisit time, and cluster of narrow spectral bands in the red and NIR wavelengths (665 nm, 705 nm, 740 nm, 783 nm, 842.5, and 865 nm) provides an excellent option to complement the coarser spatial sensors, such as MERIS, MODIS, and OLCI. This has become especially important for quantifying water quality in the thousands of smaller inland lakes that the coarser resolution imagers cannot resolve. A total of 24 Sentinel-2 algorithms were identified in the literature: 11 designed for chlorophyll a, four for phycocyanin or cyanobacteria, and nine for turbidity (Table 3). Additionally, Sentinel-2 is now considered a constellation with two identical imagers in operation, reducing the revisit time to only five days. It does not offer daily coverage and may still be hindered by cloud cover but is an improvement for moderate resolution optical imagers. Sentinel-2 is available at no cost through the US Geologic Survey (USGS) or ESA with many images already geometrically and atmospherically corrected, decreasing barriers for analytical applications, and subsequently increasing the ability of this imagery to be directly incorporated into monitoring programs.

Table 3. Sentinel-2 MSI empirically based algorithms.

Year	Parameter	Algorithm/Band Combination	Reference
2003	chl-a	$(Rrs(672)^{-1} - Rrs(715)^{-1}) * Rrs(757)$	Gitelson et al. 2003 Johansen et al. 2019
2006	chl-a	$\frac{[\mathrm{Lw}(510)/\mathrm{Lw}(555) - \mathrm{Lw}(443)]}{[\mathrm{Lw}(510)/\mathrm{Lw}(555) + \mathrm{Lw}(443)]}$	Ahn and Shanmugam 2006 Acheampong 2018
2009	chl-a	$\frac{Rrs(681)}{Rrs(665)}$	Amin et al. 2009 Johansen et al. 2019
2010	chl-a	$\frac{Rrs(857) - Rrs(644)}{Rrs(458) + Rrs(529)}$	Alawadi 2010 Johansen et al. 2019
2012	chl-a	$\frac{Rrs(709) - Rrs(665)}{Rrs(709) + Rrs(665)}$	Mishra and Mishra 2012 Beck et al. 2016 Johansen et al. 2019
2016	chl-a	$Rrs(560) - Rrs(665) + \left(Rrs(490) + Rrs(665)\right)$	Beck et al. 2016
2016	chl-a	$\frac{Rrs(705)}{Rrs(665)}$	Beck et al. 2016

Year	Parameter	Algorithm/Band Combination	Reference
2016	chl-a	$(Rrs(665)^{-1} - Rrs(705)^{-1}) * Rrs(865)$	Beck et al. 2016
2016	chl-a	$Rrs(704) - \frac{Rrs(665) + Rrs(740)}{2}$	Toming et al. 2016
2019	chl-a	$Log\frac{Rrs(490)}{Rrs(555)}$	Poddar et al. 2019
2019	chl-a	$Log\frac{Rrs(443)}{Rrs(555)}$	Poddar et al. 2019
2004	PC	$Rrs(709) - Rrs(681) - \left(Rrs(753) - Rrs(681)\right) * \left(\frac{709 - 681}{753 + 681}\right)$	Gower et al. 2004 Johansen et al. 2019
2008	PC	$Rrs(681) - Rrs(665) - \left(Rrs(709) - Rrs(665)\right) * \left(\frac{681 - 665}{709+665}\right)$	Wynne et al. 2008 Kudela et al. 2015 Johansen et al. 2019
2009	PC	$\frac{Rrs(686) - Rrs(658)}{Rrs(686) + Rrs(658)}$	Amin et al. 2009 Johansen et al. 2019
2017	PC	$\frac{Rrs(736)}{Rrs(665)}$	Beck et al 2017
1980	Turb	$Rrs(658)$	Moore 1980 Johansen et al. 2019
1991	Turb	$\frac{Rrs(658)}{Rrs(458)}$	Lathrop et al. 1991 Johansen et al. 2019
1992	Turb	$Rrs(857)$	Schiebe et al. 1992 Johansen et al. 2019
2002	Turb	$\frac{Rrs(857)}{Rrs(658)}$	Doxaran et al. 2002 Johansen et al. 2019
2006	Turb	$\frac{Rrs(658)}{Rrs(558)}$	Bowers and Binding 2006 Johansen et al. 2019
2009	Turb	$\frac{Rrs(857)}{Rrs(558)}$	Chipman et al. 2009 Johansen et al. 2019
2009	Turb	$\frac{Rrs(558) + Rrs(658)}{Rrs(458)}$	Frohn and Autrey 2009 Beck et al. 2018
2018	Turb	$\frac{Rrs(558) + Rrs(658)}{Rrs(444)}$	Beck et al. 2018

Year	Parameter	Algorithm/Band Combination	Reference
2018	Turb	$\frac{Rrs(658)}{Rrs(444)}$	Beck et al. 2018

2.3 Landsat-8 OLI

The USGS Landsat Program has been developing Earth Observing (EO) satellites and providing access to their imagery since 1972 (USGS 2007). For nearly fifty years, the Landsat missions (Landsat 1 - 8) have been used globally for a variety of remote sensing-based research (Masek et al. 2002; Wulder et al. 2019). As such, water quality algorithms have been developed since the earliest Landsat missions, but the latest, Landsat-8 OLI, was the primary focus for this review. Landsat-8's Operational Land Imager (OLI) has a spatial resolution of 30 m and contains nine spectral bands, but only bands 1-5 (443 nm – 865 nm) are utilized for HAB detection (USGS 2019). It currently has a revisit time of 16 days, but once Landsat-9 is operational in offsetting orbit to Landsat-8, the revisit time will be reduced to eight days. A total of 32 Landsat algorithms were found in the literature with 18 chlorophyll a algorithms, 1 phycocyanin, and 13 turbidity algorithms (Table 4). However, Landsat's wide spectral bands are not well-suited for aquatic studies in general and less suited for the narrow spectral bands required to accurately detect and quantify HAB-specific pigments, such as chlorophyll a and phycocyanin.

Table 4. Landsat-8 OLI empirically based algorithms.

Year	Parameter	Algorithm/Band Combination	Reference
1993	chl-a	$\frac{MSS(6)}{MSS(4)} + MSS(5) + MSS(6)$	Gitelson et al. 1993
1995	chl-a	$\frac{\mathrm{TM}(1) - \mathrm{TM}(3)}{TM(2)}$	Mayo et al. 1995 Brivio et al. 2001
1996	chl-a	$Log\frac{TM(3)}{TM(1)}$	Gitelson et al. 1996
2001	chl-a	$Ln(TM1) - Ln(TM2)$	Brivio et al. 2001
2001	chl-a	$Log\frac{TM(1)}{TM(2)}$	Östlund et al. 2001
2004	chl-a	$Log\frac{TM(2)}{TM(3)}$	Hellweger et al. 2004
2005	chl-a	$\frac{Log\ ETM(1)}{Log\ ETM(3)}$	Han and Jordan 2005

Year	Parameter	Algorithm/Band Combination	Reference
2007	chl-a	$\frac{TM(4)}{TM(3)}$	Duan et al. 2007
2007	chl-a	$\frac{Rrs(458) - Rrs(644)}{Rrs(529)}$	Kneubuhler et al. 2007 Johansen et al. 2019
2010	chl-a	$\frac{Rrs(857) - Rrs(644)}{Rrs(458) + Rrs(529)}$	Alawadi 2010 Johansen et al. 2019
2016	chl-a	$\frac{Rrs(660) - Rrs(605)}{Rrs(660) + Rrs(605)}$	Beck et al. 2016
2016	chl-a	$\frac{Rrs(660) - Rrs(605)}{Rrs(480) + Rrs(545)}$	Beck et al. 2016
2016	chl-a	$Rrs(545) - Rrs(605) + \left(Rrs(480) - Rrs(605)\right)$	Beck et al. 2016
2016	chl-a	$Rrs(545) - Rrs(605) + \left(Rrs(425) - Rrs(605)\right)$	Beck et al. 2016
2016	chl-a	$\frac{Rrs(660)}{Rrs(605)}$	Beck et al. 2016
2016	chl-a	$\frac{Rrs(480) - Rrs(605)}{Rrs(545)}$	Beck et al. 2016
2019	chl-a	$Log\frac{Rrs(490)}{Rrs(555)}$	Poddar et al. 2019
2019	chl-a	$Log\frac{Rrs(443)}{Rrs(555)}$	Poddar et al. 2019
2017	PC	$Rrs(530) - Rrs(640) + \left(Rrs(430) - Rrs(640)\right)$	Beck et al. 2017
1990	Turb	$Rrs(658)$	Moore 1980 Johansen et al. 2019
1991	Turb	$\frac{Rrs(658)}{Rrs(458)}$	Lathrop et al. 1991 Johansen et al. 2019
1992	Turb	$Rrs(857)$	Schiebe et al. 1992 Johansen et al. 2019
2001	Turb	$\frac{TM(1) - TM(4)}{TM(3) - TM(4)}$	Härmä et al. 2001
2002	Turb	$\frac{Rrs(857)}{Rrs(658)}$	Doxaran et al. 2002 Johansen et al. 2019
2004	Turb	$\frac{ETM(3)}{ETM(2)}$	Vincent et al. 2004

Year	Parameter	Algorithm/Band Combination	Reference
2005	Turb	TM3	Brezonik et al. 2005 Kallio et al. 2008
2006	Turb	$\frac{Rrs(658)}{Rrs(558)}$	Bowers and Binding 2006 Johansen et al. 2019
2007	Turb	$\frac{Rrs(558)+Rrs(658)}{Rrs(458)}$	Frohn and Autrey 2007 Beck et al. 2018
2009	Turb	$\frac{Rrs(857)}{Rrs(558)}$	Chipman et al. 2009 Johansen et al. 2019
2018	Turb	$Rrs(530) - Rrs(640) + (Rrs(430) - Rrs(640))$	Beck et al. 2018
2018	Turb	$\frac{Rrs(558)+Rrs(658)}{Rrs(444)}$	Beck et al. 2018
2018	Turb	$\frac{Rrs(658)}{Rrs(444)}$	Beck et al. 2018

2.4 MODIS

The MODIS sensor is currently operational onboard two National Aeronautics and Space Administration’s (NASA) satellites, Terra launched in 1999 and Aqua launched in 2002. MODIS contains 36 spectral bands with spatial resolutions ranging from 250 m to 1000 m and a revisit time of 1-2 days (NASA n.d.). Eight MODIS algorithms were identified, including five chlorophyll a, three turbidity, and zero phycocyanin algorithms (Table 5). Furthermore, even a simple band ratio between the two 250 m spectral bands (645 nm and 858 nm) have been useful for estimating both turbidity and chlorophyll-a (Beck et al. 2016; Beck et al. 2018). Unfortunately, MODIS has not been a primary focus for HAB monitoring because most of its important spectral bands have very coarse spatial resolutions (1,000 m), which severely limits the application of this sensor to large lakes or the open ocean. Nevertheless, research has shown that MODIS has been successful at detecting HABs with the coarse resolution sensors. It also served a role in bridging the operational gap between the decommissioning of Envisat (MERIS) in 2011 and the launch of Sentinel-3 (OLCI) in 2016.

Table 5. MODIS empirically based algorithms.

Year	Parameter	Algorithm/Band Combination	Reference
2009	chl-a	$\frac{Rrs(443)}{Rrs(551)}$	Chavula et al. 2009
2009	chl-a	$\frac{Rrs(748)}{Rrs(667)}$	Moses et al. 2009
2009	chl-a	$Ln(B2) + Ln(B9) - \frac{Ln(B3-B2)}{B(2)}$	Wu et al. 2009
2016	chl-a	$\frac{Rrs(857) - Rrs(646)}{Rrs(857) + Rrs(646)}$	Beck et al. 2016 Beck et al 2017
2016	chl-a	$\frac{Rrs(857)}{Rrs(646)}$	Beck et al. 2016
1980	Turb	$Rrs(658)$	Beck et al. 2018 Chen et al. 2007 Moore 1980
1992	Turb	$Rrs(857)$	Beck et al. 2018 Schiebe et al. 1992
2002	Turb	$\frac{Rrs(857)}{Rrs(658)}$	Beck et al. 2018 Doxaran et al. 2002

2.5 MERIS and Sentinel-3 OLCI

The MERIS imager was developed by the ESA and was onboard the now decommissioned Envisat satellite. MERIS was operational and provided coverage of the US from 2008 through 2011. The MERIS sensor had moderate spatial resolution at 300 m, 15 spectral bands, and provided revisit times of 2-3 days (ESA 1995). Unfortunately, there was a 5-yr gap between the decommissioning of MERIS and the launch of Sentinel-3 and the OLCI sensor. The Sentinel-3 program, like many recent satellite programs, is considered a constellation with two satellites currently operational and two more expected to be launched soon. The two operational Sentinel-3 satellites provide a near daily revisit time for the OLCI sensor, with a spatial resolution of 300 m (ESA 2015b). Additionally, most OLCI's spectral band centers align well with MERIS, allowing for a near seamless transfer of algorithms between the sensors (Table 1).

MERIS, and more recently OLCI, have become the primary satellite-based imagers for the detection and quantification of HABs and water quality related pigments. This is primarily due to the more robust spectral resolution coupled with the near daily revisit times, which have outweighed the higher spatial resolution imagers such as Landsat-8 and Sentinel-2. Generally, the spectral resolution of these sensors is much more conducive to distinguishing optical properties of water because of their many narrow spectral bands. A total of 62 MERIS/OLCI algorithms were identified, including 30 chlorophyll a, 21 phycocyanin, and 11 turbidity algorithms (Table 6). The algorithms for these sensors were combined for simplicity because their spectral configurations are very similar and MERIS was decommissioned in 2011. Additionally, these sensors contain a spectral band centered around 620 nm, making them capable of detecting the absorbance of phycocyanin. A limitation of these sensors is the coarse spatial resolution (~300-m pixels), which makes it difficult to resolve smaller inland water bodies and coastlines due to the lower resolution.

Table 6. MERIS and Sentinel-3 OLCI empirically based algorithms.

Year	Parameter	Algorithm/Band Combination	Reference
1993	chl-a	$Rrs(600) - Rrs(648) - Rrs(625)$	Dekker 1993 Johansen et al. 2019
2001	chl-a	$Rrs(550)$	Flink et al. 2001
2001	chl-a	$\frac{Rrs(708)}{Rrs(678)}$	Flink et al. 2001
2001	chl-a	$\frac{Rrs(708)}{Rrs(678)} + \frac{Rrs(643)}{Rrs(628)}$	Flink et al. 2001
2001	chl-a	$\frac{L(705) - L(754)}{L(665) - L(754)}$	Härmä et al. 2001
2001	chl-a	$\frac{L(702)}{L(674)}$	Kallio et al. 2001
2002	chl-a	$\frac{L(709)}{L(665)}\ OR\ \frac{Rrs(709)}{Rrs(665)}$	Ammenberg et al. 2002 Gons et al. 2002 Kallio et al. 2003 Koponen et al. 2007 Moses et al. 2009 Beck et al. 2016
2002	chl-a	$\frac{L(700)}{L(662)} + \frac{L(781)}{L(781)}$	Koponen et al. 2002
2003	chl-a	$\frac{L(620)}{L(490)} + \frac{L(560)}{L(510)}$	Floricioiu et al. 2003
2003	chl-a	$(Rrs(672)^{-1} - Rrs(715)^{-1}) * Rrs(757)$	Gitelson et al. 2003 Gitelson et al. 2009 Johansen et al. 2019

Year	Parameter	Algorithm/Band Combination	Reference
2004	chl-a	$\frac{L(665)}{L(560)}$	Floricioiu et al. 2004
2005	chl-a	$\frac{L(560)}{L(665)}$	Candiani et al. 2005
2005	chl-a	$\frac{L(440)-L(780)}{L(780)-L(700)}$	Giardino et al. 2005
2005	chl-a	$L(489)$	Giardino et al. 2005
2007	chl-a	$\frac{Rrs(458)-Rrs(664)}{Rrs(529)}$	Kneubuhler et al. 2007 Johansen et al. 2019
2009	chl-a	$Rrs(681) - Rrs(665)$	Amin et al. 2009 Johansen et al. 2019
2009	chl-a	$(Rrs(665)^{-1} - Rrs(708)^{-1}) * Rrs(753)$	Moses et al. 2009 Le et al. 2009
2010	chl-a	$\frac{Rrs(857)-Rrs(644)}{Rrs(458)-Rrs(529)}$	Alawadi 2010 Johansen et al. 2019
2010	chl-a	$Rrs(686)-Rrs(715)+(Rrs(672)-Rrs(715)) * (\frac{715 - 672}{686+672})$	Zhao et al. 2010 Johansen et al. 2019
2012	chl-a	$Rrs(665)^{-1} * Rrs(708)$	Moses et al. 2012
2012	chl-a	$(Rrs(665)^{-1} * Rrs(708)) * Rrs(753)$	Moses et al. 2012 Augusto-silva et al. 2014
2016	chl-a	$\frac{Rrs(658)-Rrs(458)}{Rrs(658)+Rrs(458)}$	Beck et al 2017
2016	chl-a	$-1 * (Rrs(681) - Rrs(665) + (Rrs(709) - Rrs(665)))$	Beck et al. 2016
2016	chl-a	$Rrs(709) - Rrs(681) + (Rrs(753) - Rrs(681))$	Beck et al. 2016
2016	chl-a	$Rrs(709) - Rrs(753) + (Rrs(681) - Rrs(753))$	Beck et al. 2016
2016	chl-a	$\frac{Rrs(709)-Rrs(665)}{Rrs(709)+Rrs(665)}$	Beck et al. 2016
2016	chl-a	$Rrs(665)^{-1} - Rrs(709)^{-1} * Rrs(761)$	Beck et al. 2016
2016	chl-a	$Rrs(529) - Rrs(644) + (Rrs(458) - Rrs(644))$	Beck et al. 2016

Year	Parameter	Algorithm/Band Combination	Reference
2016	chl-a	$Rrs(529) - (Rrs(644) + (Rrs(429) - Rrs(644)))$	Beck et al. 2016
2016	chl-a	$\frac{Rrs(658) - Rrs(444)}{Rrs(658) + Rrs(444)}$	Beck et al. 2016
2000	PC	$\frac{Rrs(650)}{Rrs(625)}$	Schalles and Yacobi 2000 Beck et al. 2017 Johansen et al. 2019
2003	PC	$\frac{Rrs(714)}{Rrs(672)}$	Dall'Olmo et al. 2003 Johansen et al. 2019
2004	PC	$Rrs(709) - Rrs(681) - (Rrs(753) - Rrs(681) * (\frac{709 - 681}{753 + 681}))$	Gower et al. 2004 Johansen et al. 2019
2005	PC	$\frac{Rrs(709)}{Rrs(620)}$	Simis et al. 2005 Simis et al. 2007 Johansen et al. 2019
2005	PC	$\frac{Rrs(720)}{Rrs(620)}$	Simis et al. 2005 Beck et al 2017
2008	PC	$Rrs(615)^{-1} - Rrs(600)^{-1} - Rrs(725)$	Hunter et al. 2008 Johansen et al. 2019
2008	PC	$-1 * (Rrs(681) - Rrs(665) - \left(Rrs(709) - Rrs(665)\right) * \left(\frac{681 - 665}{709+665}\right))$	Wynne et al. 2008 Kudela et al. 2015 Johansen et al. 2019
2009	PC	$\frac{Rrs(686) - Rrs(658)}{Rrs(686) + Rrs(658)}$	Amin et al. 2009 Johansen et al. 2019
2009	PC	$\frac{Rrs(700)}{Rrs(600)}$	Mishra et al. 2009 Beck et al. 2017 Johansen et al. 2019
2009	PC	$\frac{Rrs(724)}{Rrs(600)}$	Mishra et al. 2009 Johansen et al. 2019
2012	PC	$\frac{Rrs(709)}{Rrs(600)}$	Mishra 2012 Johansen et al. 2019
2014	PC	$Rrs(629)^{-1} - Rrs(659)^{-1} - Rrs(724)$	Mishra and Mishra 2014 Johansen et al. 2019
2017	PC	$\frac{Rrs(707)}{Rrs(679)}$	Beck et al. 2017
2017	PC	$Rrs(644) - Rrs(629)$	Beck et al. 2017

Year	Parameter	Algorithm/Band Combination	Reference
2017	PC	$Rrs(658) - Rrs(857) + (Rrs(458) - Rrs(857))$	Beck et al. 2017
2017	PC	$Rrs(658) - Rrs(857) + (Rrs(558) - Rrs(857))$	Beck et al. 2017
2017	PC	$Rrs(658) - Rrs(857) + (Rrs(444) - Rrs(857))$	Beck et al. 2017
2017	PC	$Rrs(615) - Rrs(601) - (Rrs(644) - Rrs(601))$	Beck et al. 2017
2017	PC	$\frac{Rrs(700) - Rrs(622)}{Rrs(700) + Rrs(622)}$	Beck et al. 2017
2017	PC	$\frac{Rrs(644) - Rrs(615)}{Rrs(644) + Rrs(615)}$	Beck et al. 2017
2017	PC	$\frac{Rrs(644) - Rrs(629)}{Rrs(644) + Rrs(629)}$	Beck et al. 2017
1980	Turb	$Rrs(658)$	Moore 1980 Johansen et al. 2019
1991	Turb	$\frac{Rrs(658)}{Rrs(458)}$	Lathrop et al. 1991 Johansen et al. 2019
1992	Turb	$Rrs(857)$	Schiebe et al. 1992 Johansen et al. 2019
2001	Turb	$L(710)$	Kallio et al. 2001 Koponen et al. 2002
2002	Turb	$\frac{Rrs(857)}{Rrs(658)}$	Doxaran et al. 2002 Johansen et al. 2019
2006	Turb	$\frac{Rrs(658)}{Rrs(558)}$	Bowers and Binding 2006 Johansen et al. 2019
2009	Turb	$\frac{Rrs(558) + Rrs(658)}{Rrs(458)}$	Frohn and Autrey 2007 Beck et al. 2018
2009	Turb	$\frac{Rrs(857)}{Rrs(558)}$	Chipman et al. 2009 Johansen et al. 2019
2018	Turb	$\frac{Rrs(864)}{Rrs(665)}$	Beck et al. 2018
2018	Turb	$\frac{Rrs(558) + Rrs(658)}{Rrs(444)}$	Beck et al. 2018
2018	Turb	$\frac{Rrs(658)}{Rrs(444)}$	Beck et al. 2018

3 Discussion

This literature review identified 158 novel and modified algorithms for the estimation of three primary water quality parameters (chlorophyll-a, phycocyanin, and turbidity) and six well-established satellite imagers (WorldView-2, Sentinel-2, Landsat-8, MODIS, MERIS, and Sentinel-3). Given the limited number of HAB-specific spectral features detectable by this suite of sensors and that each has a limited number of spectral bands, the development of novel empirically-based algorithms has plateaued. This was evident by the fact that four algorithm types accounted for roughly 65% of the total algorithms identified across all sensors. The top four algorithm types were the two-band difference algorithms (2BDA), the fluorescence line height (FLH), the normalized difference chlorophyll index algorithms (NDCI), and the three-band difference algorithms (3BDA), representing 35.4%, 14%, 9.5%, and 6.3% of the total algorithms, respectively (Table 7). The distribution of algorithms by sensor was also consistent, with most algorithm development focused on 2BDA-style algorithms followed by FLH, NDCI, and 3BDA (Figure 1).

Table 7. Common algorithm types.

Algorithm	Equation
2BDA	$\frac{Rrs(Bx)}{Rrs(By)}$
FLH	$L_2 - L_1 - (L_3 - L_1)((\lambda_2 - \lambda_1)/(\lambda_3 - \lambda_1))$
NDCI	$\frac{Rrs(Bx) - Rrs(By)}{Rrs(Bx) + Rrs(By)}$
3BDA	$Rrs(Bx)^{-1}\ Rrs(By)^{-1}) * Rrs(Bz)$

However, algorithm development and the field of remote sensing continues to rapidly grow. The development of site specific and more complex algorithms, such as semi-empirical or analytical, continue to expand. Additionally, with the advent of new sensors (e.g., hyperspectral) and platforms (e.g., cubesats and unmanned aircraft systems), there will still be a need for novel and modified algorithms to keep pace with the ever-evolving field. This review aimed to compile a near-comprehensive list of empirically-based satellite algorithms to serve as a reference database to evaluate portable algorithms specific to satellite sensor type, water quality parameter, and waterbody/environmental condition combination as determined by available monitoring data and USACE district needs.

Figure 1. Frequency of algorithms by types by sensor.

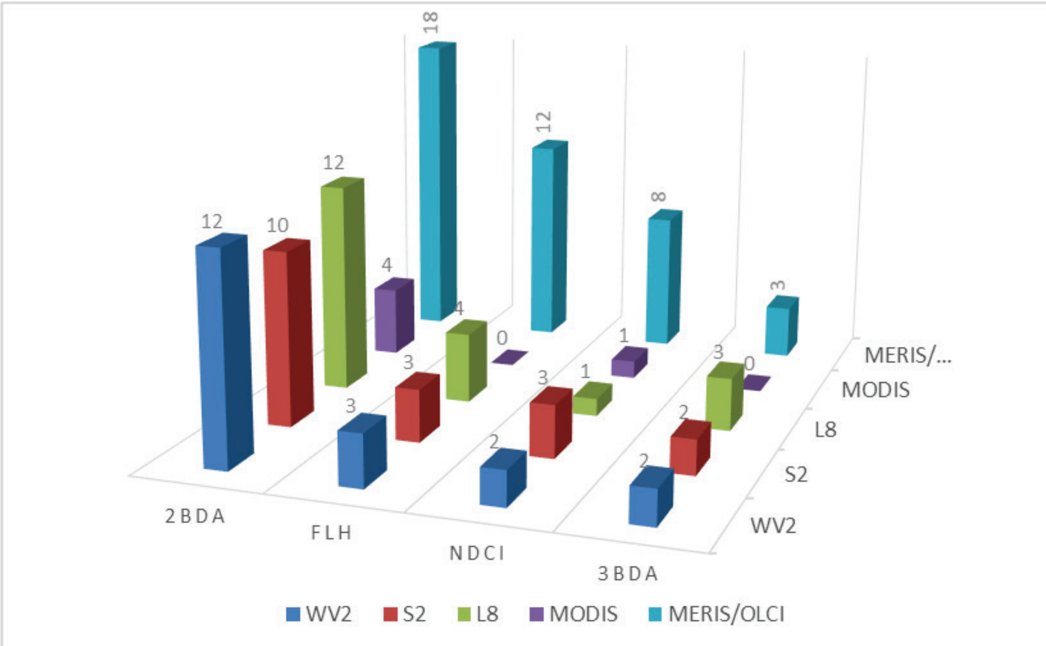

The majority of the algorithms discovered fell into one of four common algorithm families including two-band difference algorithms (2BDA) with 56, Fluorescence Line Height (FLH) with 24, Normalized Difference Chlorophyll Index (NDCI) with 15, and three-band difference algorithms (3BDA) with 10.

References

Acheampong, C. 2018. Deriving algal concentration from Sentinel-2 through a downscaling technique: A case near the intake of a desalination plant. MS Thesis. University of Twente.

Agha, R., S. Cirés, L. Wörmer, J. A. Domínguez, and A. Quesada. 2012. "Multi-scale strategies for the monitoring of freshwater cyanobacteria: reducing the sources of uncertainty." *Water Res* , *46*: 3043–3053.

Ahn, Y-H., and P. Shanmugam. 2006. "Detecting the red tide algal blooms from satellite ocean color observations in optically complex Northeast-Asia coastal waters." *Remote Sensing of Environment* 103(4): 419–37. https://doi.org/10.1016/j.rse.2006.04.007.

Alawadi, F. 2010. "Detection of surface algal blooms using the newly developed algorithm surface algal bloom index (SABI)." In *Proc. SPIE*, 7825.

Amin, R., J. Zhou, A. Gilerson, B. Gross, F. Moshary, and S. Ahmed. 2009. "Novel optical techniques for detecting and classifying toxic dinoflagellate Karenia brevis blooms using satellite imagery." *Opt. Express*, 17 (11): 1-13.

Ammenberg, P., P. Flink, T. Lindell, D. Pierson, and N. Strombeck. 2002. "Bio-optical modelling combined with remote sensing to assess water quality." *International Journal of Remote Sensing*, 23(8), 1621-1638. DOI: 10.1080/01431160110071860.

Anderson, D., M. P. Hoagland, Y. Kaoru, and A. W. White. 2000. *Estimated annual economic impact from harmful algal blooms (HABs) in the United States*. Woods Hole, MA: Woods Hole Oceanographic Institution.

Augusto-Silva, P. B., I. Ogashawara, C. F. Barbosa, L. A. S. de Carvalho, D. S. F. Jorge, C. I. Fornari, and J. L. Stech. 2014. "Analysis of MERIS reflectance algorithms for estimating chlorophyll-*a* concentration in a Brazilian reservoir." *Remote Sens*, *6*: 11689-11707. https://doi.org/10.3390/rs61211689

Beck, R., S. Zhan, H. Liu, S. Tong, B. Yang, M. Xu, Z. Ye, Y. Huang, S. Shu, Q. Wu, S. Wang, K. Berling, A. Murray, E. Emery, M. Reif, J. Harwood, J. Young, C. Nietch, D. Macke, M. Martin, G. Stillings, R. Stumpf, and H. Su. 2016. "Comparison of satellite reflectance algorithms for estimating chlorophyll-a in a temperate reservoir using coincident hyperspectral aircraft imagery and dense coincident surface observations." *Remote Sens. Environ.*, 178: 15-30.

Beck, R., M. Xu, S. Zhan, H. Liu, R. A. Johansen, S. Tong, B. Yang, S. Shu, Q. Wu, S. Wang, K. Berling, A. Murray, E. Emery, M. Reif, J. Harwood, J. Young, M. Martin, G. Stillings, R. Stumpf, H. Su, Z. Ye, and Y. Huang. 2017. "Comparison of satellite reflectance algorithms for estimating phycocyanin values and cyanobacterial total biovolume in a temperate reservoir using coincident hyperspectral aircraft imagery and dense coincident surface observations." *Remote Sens.*, 9: 538.

Beck, R., M. Xu, S. Zhan, R. A. Johansen, H. Liu, S. Tong, B. Yang, S. Shu, Q. Wu, S. Wang, K. Berling, A. Murray, E. Emery, M. Reif, J. Harwood, J. Young, C. Nietch, M. Martin, G. Stillings, R. Stumpf, H. Su, Z. Ye, and Y. Huang. 2018. "Comparison of satellite reflectance algorithms for estimating turbidity and cyanobacterial concentrations in productive freshwaters using hyperspectral aircraft imagery and dense coincident surface observations." *Journal of Great Lakes Research* 45(3): 413-433.

Bowers, D. G., and C. E. Binding. 2006. "The optical properties of mineral suspended particles: A review and synthesis." *Estuarine Coastal and Shelf Science* 67 (1–2): 219–230. doi:10.1016/j.ecss.2005.11.010.

Brezonik, P., K. D. Menken, and M. Bauer. 2005. "Landsat-based remote sensing of lake water quality characteristics, including chlorophyll and colored dissolved organic matter (CDOM)." *Lake and Reservoir Management*, 21(4), 373-382. DOI: 10.1080/07438140509354442.

Brivio, P. A., C. Giardino, and E. Zilioli. 2001. "Determination of chlorophyll concentration changes in Lake Garda using an image-based radiative transfer code for Landsat TM images." *International Journal of Remote Sensing*, 22(2-3): 487-502. DOI: 10.1080/014311601450059.

Candiani, G., D. Floricioiu, C. Giardino, and H. Rott. 2005. "Monitoring Water Quality of the Perialpine Italian lake Garda through Multi-temporal MERIS data." In *MERIS/(A)ATSR User Workshop*, 26–30.

Carvalho, G. A., P. J. Minnett, L. E. Fleming, V. F. Banzon, and W. Baringer. 2010. "Satellite remote sensing of harmful algal blooms: A new multi-algorithm method for detecting the Florida Red Tide (Karenia brevis)." *HARMFUL ALGAE*, 9(5): 440-448.

Chipman, J. W., L. G. Olmanson, and A. A. Gitelson. 2009. Remote sensing methods for lake management: A guide for resource managers and decision-makers. North American Lake Management Society. University of Minnesota. https://www.worldcat.org/title/remote-sensing-methods-for-lake-management-a-guide-for-resource-managers-and-decision-makers/oclc/752201814?referer=di&ht=edition.

Clark, J. M., B. A. Schaeffer, J. A. Darling, E. A. Urquhart, J. M. Johnston, A. R. Ignatius, M. H. Myer, K. A. Loftin, P. J. Werdell, and R. P. Stumpf. 2017. "Satellite monitoring of cyanobacterial harmful algal bloom frequency in recreational waters and drinking water sources." *Ecological Indicators*, 80: 84-95. https://doi.org/10.1016/j.ecolind.2017.04.046.

Coffer, M. M., B. A. Schaeffer, J. A. Darling, E. A. Urquhart, and W. B. Salls. 2020. "Quantifying national and regional cyanobacterial occurrence in US lakes using satellite remote sensing." *Ecological Indicators*, 111: 105976. https://doi.org/10.1016/j.ecolind.2019.105976.

Dall'Olmo, G., A. A. Gitelson, and D. C. Rundquist. 2003. "Towards a unified approach for remote estimation of chlorophyll-a in both terrestrial vegetation and turbid productive waters." *Geophys. Res. Lett.*, 30: 1938. doi:10.1029/2003GL018065.

Davis, C. O., M. Kavanaugh, R. Letelier, W. P. Bissett, and D. Kohler. 2007. "Spatial and spectral resolution considerations for imaging coastal waters." In *Proc. SPIE 2007*, 6680. doi: 10.1117/ 12.734288.

Dekker, A. G. 1993. *Detection of Optical Water Quality Parameters for Eutrophic Waters by High Resolution Remote Sensing*. Ph.D. Dissertation, Vrije University Amsterdam.

DigitalGlobe. 2009. WorldView-2 Overview. https://content.satimagingcorp.com.s3.amazonaws.com/static/satellite-sensor-specification/WorldView-2-PDF-Download.pdf.

Dogliotti, A. I., K. G. Ruddick, B. Nechad, D. Doxaran, and E. Knaeps. 2015. "A single algorithm to retrieve turbidity from remotely sensed data in all coastal and estuarine waters." *Remote Sens. Environ.*, 156: 157-168.

Dokulil, M. T., and K. Teubner. 2000. "Cyanobacterial dominance in lakes." *Hydrobiologia,* 438(1-3): 1–12.

Doxaran, D., J. M. Froidefond, and P. Castaing. 2002. "A reflectance band ratio used to estimate suspended matter concentrations in sediment dominated coastal waters." *Remote Sens.*, 23: 5079-5085.

Duan, H., Y. Zhang, B. Zhang, K. Song, and Z. Wang. 2007. "Assessment of chlorophyll-*a* concentration and trophic state for Lake Chagan using landsat tm and field spectral data." *Environ Monit Assess,* 129**:** 295–308. https://doi.org/10.1007/s10661-006-9362-y.

ESA (European Space Agency). 1995. MERIS: The Medium Resolution Imaging Spectrometer. *SP-1184*. https://earth.esa.int/eogateway/documents/20142/37627/MERIS-The-Medium-Resolution-Imaging-Spectrometer.pdf

ESA (European Space Agency). 2015a. *Sentinel-2 User Handbook*. https://sentinel.esa.int/documents/247904/685211/Sentinel-2_User_Handbook.

ESA (European Space Agency). 2015b. *Sentinel-3 Data Access and Products*. https://sentinels.copernicus.eu/documents/247904/1848151/Sentinel-3_OLCI_Data_Access_and_Products.pdf.

Flink P., L. T. Lindell, and C. Östlund. 2001. "Statistical analysis of hyperspectral data from two Swedish lakes." *Science of The Total Environment*, 268(1–3): 155-169. https://doi.org/10.1016/S0048-9697(00)00686-0.

Floricioiu, D., C. Riedl, H. Rott, and E. Rott. 2003. "Envisat MERIS capabilities for monitoring the water quality of Perialpine Lakes." In *IGARSS 2003, IEEE International Geoscience and Remote Sensing Symposium. Proceedings (IEEE Cat. No.03CH37477),* Toulouse, France, pp. 2134-2136, doi: 10.1109/IGARSS.2003.1294363.

Floricioiu, D., H. Rott, E. Rott, M. Dokulil, and C. Defrancesco. 2004. "Retrieval of limnological parameters of perialpine lakes by means of MERIS data." In *Envisat & ERS Symposium, Salzburg, Austria*, 6-10 September. ISBN: 92-9092-883-2.

Frohn, R. C., and B. C. Autrey. 2007. "Water quality assessment in the Ohio River using new indices for turbidity and chlorophyll-a with Landsat-7 Imagery." In *SWIMS Conference*, Chicago, IL, January 30 - February 01.

Giardino, C., G. Candiani, and E. Zilioli. 2005. "Detecting Chlorophyll-a in Lake Garda Using TOA MERIS Radiances." *Photogrammetric Engineering & Remote Sensing*, 71(9): 1045-1051. https://doi.org/10.14358/PERS.71.9.1045

Gitelson, A., G. Garbuzov, F. Szilagyi, K. H. Mittenzwey, A. Karnieli, and A. Kaiser. 1993. "Quantitative remote sensing methods for real-time monitoring of inland waters quality." *Int. J. Remote Sens.*, 14: 1269-1295.

Gitelson, A., Y. Z. Yacobi, A. Karnieli, and A. Kress. 1996. "Reflectance spectra of polluted marine waters in Haifa Bay, Southeastern Mediterranean: Features and applications for remote estimation of chlorophyll concertation." *Isr. J. Earth Sci.*, 45: 127-136.

Gitelson, A., Y. Gritz, and M. N. Merzlyak. 2003. "Relationships between leaf chlorophyll content and spectral reflectance and algorithms for non-destructive chlorophyll assessment in higher plant leaves." *J. Plant Phys.*, 160: 271-282.

Gitelson, A., D. Gurlin, W. J. Moses, and T. Barrow. 2009. "A bio-optical algorithm for the remote estimation of the chlorophyll-a concentration in case waters." *Environ. Res. Lett.*, 4: 045003. https://doi.org/10.1088/1748-9326/4/4/045003

Glazer, A. N., S. Fang, and D. M. Brown. 1973. "Spectroscopic properties of c-phycocyanin and of its α and β subunits*." *The Journal of Biological Chemistry*, 248(16): 5679-5685. https://doi.org/10.1016/S0021-9258(19)43559-X.

Gons, H. J., M. Rijkeboer, K. G. Ruddick. 2002. "A chlorophyll-retrieval algorithm for satellite imagery (Medium Resolution Imaging Spectrometer) of inland and coastal waters." *Journal of Plankton Research*, 24(9): 947–951. https://doi.org/10.1093/plankt/24.9.947

Gower, J. F. R., L. Brown, and G. A. Borstad. 2004. "Observation of chlorophyll fluorescence in west coast waters of Canada using the MODIS satellite sensor." *Canadian Journal of Remote Sensing*, 30(1): 17-25. DOI: 10.5589/m03-048

Han, L., and K. J. Jordan. 2005. Estimating and mapping chlorophyll-*a* concentration in Pensacola Bay, Florida using Landsat ETM+ data." *International Journal of Remote Sensing*, 26(23): 5245-5254. DOI: 10.1080/01431160500219182

Härmä, P., J. Vepsäläinen, T. Hannonen, T. Pyhälahti, J. Kämäri, K. Kallio, K. Eloheimo, and S. Koponen. 2001. "Detection of water quality using simulated satellite data and semi-empirical algorithms in Finland." *Science of The Total Environment*, 268(1-3): 107-121. https://doi.org/10.1016/S0048-9697(00)00688-4

Hellweger, F. L., P. Schlosser, U. Lall, and J. K. Weissel. 2004. "Use of satellite imagery for water quality studies in New York Harbor." *Estuarine, Coastal and Shelf Science*, 61(3): 437-448. https://doi.org/10.1016/j.ecss.2004.06.019

Hu, C., F. E. Muller-Karger, C. Taylor, K. L Carder, C. Kelble, E. Johns, and C. A. Heil. 2005. "Red tide detection and tracing using MODIS fluorescence data: A regional example in SW Florida coastal waters." *Remote Sens. Environ.*, 97: 311–321.

Hunter, P. D., A. N. Tyler, N. J. Willby, and D. J. Gilvear. 2008. "The spatial dynamics of vertical migration by Microcystis aeruginosa in a eutrophic shallow lake: A case study using high spatial resolution time-series airborne remote sensing." *Limn. Oceanogr.* 53: 2391-2406

Johansen, R., R. Beck, J. Nowosad, C. Nietch, M. Xu, S. Shu, B. Yang, H. Liu, E. Emery, M. Reif, J. Harwood, J. Young, D. Macke, M. Martin, G. Stillings, R. Stumpf, and H. Su. 2018. "Evaluating the portability of satellite derived chlorophyll-a algorithms for temperate inland lakes using airborne hyperspectral imagery and dense surface observations." *Harmful Algae*, 76: 35-46. https://doi.org/10.1016/j.hal.2018.05.001

Johansen, R., M. Reif, E. Emery, J. Nowosad, R. A. Beck, M. Xu, and H. Liu. 2019. *Waterquality: An open-source r package for the detection and quantification of cyanobacterial harmful algal blooms and water quality.* ERDC/EL TR-19-20. Vicksburg, MS: U.S. Army Engineer Research and Development Center. https://hdl.handle.net/11681/35053

Kallio, K., T. Kutser, T. Hannonen, S. Koponen, J. Pulliainen, J. Vepsäläinen, and T. Pyhälahti. 2001. "Retrieval of water quality from airborne imaging spectrometry of various lake types in different seasons." *Science of The Total Environment*, 268(1-3): 59-77. https://doi.org/10.1016/S0048-9697(00)00685-9

Kallio, K., S. Koponen, and J. Pulliainen. 2003. "Feasibility of airborne imaging spectrometry for lake monitoring—a case study of spatial chlorophyll *a* distribution in two meso-eutrophic lakes." *International Journal of Remote Sensing*, 24(19): 3771-3790. DOI: 10.1080/0143116021000023899

Kallio, K., J. Attila, P. Härmä, S. Koponen, J. Pulliainen, U-M. Hyytiäinen, and T. Pyhälahti. 2008. "Landsat ETM+ Images in the Estimation of Seasonal Lake Water Quality in Boreal River Basins." *Environmental Management,* 42**:** 511–522. https://doi-org.erdclibrary.idm.oclc.org/10.1007/s00267-008-9146-y

Koponen, S., J. Pulliainen, K. Kallio, and M. Hallikainen. 2002. "Lake water quality classification with airborne hyperspectral spectrometer and simulated MERIS data." *Remote Sensing of Environment*, 79(1): 51-59. https://doi.org/10.1016/S0034-4257(01)00238-3

Koponen, S., J. Attila, J. Pulliainen, K. Kallio, T. Pyhälahti, A. Lindfors, K. Rasmus, and M. Hallikainen. 2007. "A case study of airborne and satellite remote sensing of a spring bloom event in the Gulf of Finland." *Continental Shelf Research*, 27(2): 228-224. https://doi.org/10.1016/j.csr.2006.10.006

Kudela, R., M. Sherry, L. Palacios, D. C. Austerberry, E. K. Accorsi, L. S. Guild, and J. Torres-Perez. 2015. "Application of hyperspectral remote sensing to cyanobacterial blooms in inland waters." *Remote Sens. Environ.*, 167: 1-10. https://doi.org/10.1016/j.rse.2015.01.025

Kutser, T., J. Hedley, C. Giardino, C. Roelfsema, and V. E. Brando. 2020. "Remote sensing of shallow waters – A 50 year retrospective and future directions." *Remote Sens. Environ.* , *240*: 111619.

Lathrop, R. G., T. M. Lillesand, and B. S. Yandell. 1991. "Testing the utility of simple multi-date Thematic Mapper calibration algorithms for monitoring turbid inland waters." *International Journal of Remote Sensing*, 2045-2063. https://doi.org/10.1080/01431169108955235

Le, C., Y. Li, Y. Zha, D. Sun, C. Huang, and H. Lu. 2009. "A four-band semi-analytical model for estimating chlorophyll a in highly turbid lakes: The case of Taihu Lake, China." *Remote Sensing of Environment*, 113(6): 1175-1182. https://doi.org/10.1016/j.rse.2009.02.005

Lekki, J., E. Deutsch, M. Sayers, K. Bosse, R. Anderson, R. Tokars, and R. W. Sawtell. 2019. "Determining remote sensing spatial resolution requirements for the monitoring of harmful algal blooms in the Great Lakes." *Journal of Great Lakes Research*, 45(3): 434-443. http://dx.doi.org/10.1016/j.jglr.2019.03.014

Li, L., and K. Song. 2017. "Bio-optical modeling of phycocyanin." In *bio-optical modeling and remote sensing of inland waters*; Elsevier: Amsterdam, The Netherlands 233–262, ISBN 978-0-12-804644-9.

Linkov, I., F. K. Satterstrom, D. Loney, and J. A. Steevans. 2009. *The impact of harmful algal blooms on USACE operations*. ERDC/TN ANSRP-09-1. Vicksburg, MS: U.S. Army Engineer Research and Development Center. https://apps.dtic.mil/sti/citations/ADA494537

Lunetta, R. S., B. A. Schaeffer, R. P. Stumpf, D. Keith, S. A. Jacobs, and M. S. Murphy. 2015. "Evaluation of cyanobacteria cell count detection derived from MERIS imagery across the eastern USA." *Remote Sens. Environ., 157*: 24–34.

Masek, J. G., M. A. Wulder, B. Markham, J. McCorkel, C. J. Crawford, J. Storey, D. T. Jenstrom. 2002. "Landsat 9: Empowering open science and applications through continuity." *Remote Sensing of Environment*, 248-111968. https://doi.org/10.1016/j.rse.2020.111968

Matthews, M. W. 2011. "A current review of empirical procedures of remote sensing in inland and near-coastal transitional waters." *International Journal of Remote Sensing*, 32: 6855– 6899.

Matthews, M. W., and D. Odermatt. 2015. "Improved algorithm for routine monitoring of cyanobacteria and eutrophication in inland and near-coastal waters." *Remote Sens. Environ., 156*: 374–382.

Mayo M., A. Gitelson, Y. Z. Yacobi, and Z. Ben-avraham. 1995. "Chlorophyll distribution in Lake Kinneret determined from Landsat Thematic Mapper data." *International Journal of Remote Sensing*, 16(1): 175-182. DOI: 10.1080/01431169508954386

Mishra, S., D. R. Mishra, and W. M. Schluchter. 2009. "A novel algorithm for predicting PC concentrations in cyanobacteria: A proximal hyperspectral remote sensing approach." *Remote Sens.*, 1: 758–775.

Mishra, S. 2012. *Remote sensing of cyanobacteria in turbid productive waters*. PhD Dissertation. Mississippi State University.

Mishra, S., and D. R. Mishra. 2012. "Normalized difference chlorophyll index: A novel model for remote estimation of chlorophyll-a concentration in turbid productive waters." *Remote Sens. Environ.*, 117: 394-406.

Mishra, S., and D. R. Mishra. 2014. "A novel remote sensing algorithm to quantify phycocyanin in cyanobacterial algal blooms." *Environ. Res. Lett., 9*: 114003.

Mishra, D. R., I. Ogashawara, A. Gitelson. 2017. *Bio-optical Modeling and Remote Sensing of Inland Waters*. ISBN 9780128046548.

Mittenzwey, K. H., S. Ullrich, A. A. Gitelson, K. Y. Kondratiev. 1992. "Determination of chlorophyll a of inland waters on the basis of spectral reflectance." *Limnology and Oceanography*, 37: 147-149.

Moore, G. K. 1980. "Satellite remote sensing of water turbidity." *Hydrological Sciences*, 25(4): 407-422.

Moses, W. J., A. A. Gitelson, S. Berdnikov, and V. Povazhnyy. 2009. "Estimation of chlorophyll-*a* concentration in case II waters using MODIS and MERIS data—successes and challenges." *Environ. Res. Lett.,* 4: 045005. https://doi.org/10.1088/1748-9326/4/4/045005

Moses, W. J., A. A. Gitelson, S. Berdnikov, V. Saprygin, and V. Povazhnyi. 2012. "Operational MERIS-based NIR-red algorithms for estimating chlorophyll-a concentrations in coastal waters - The Azov Sea case study." *Remote Sensing of Environment*, 121: 118-124. https://doi.org/10.1016/j.rse.2012.01.024

NASA (National Aeronautics and Space Administration). Moderate-resolution Imaging Spectroradiometer (MODIS): NASA's Earth Observing System. N.d. https://modis.gsfc.nasa.gov/about/media/modis_brochure.pdf

Östlund, C., P. Flink, N. Strömbeck, D. Pierson, and T. Lindell. 2001. "Mapping of the water quality of Lake Erken, Sweden, from Imaging Spectrometry and Landsat Thematic Mapper." *Science of The Total Environment*, 268(1-3): 139-154. https://doi.org/10.1016/S0048-9697(00)00683-5

Petus, C., G. Chust, F. Gohin, D. Doxaran, J-M. Froidefond, and Y. Sagarminaga. 2010. "Estimating turbidity and total suspended matter in the Adour River plume (South Bay of Biscay) using MODIS 250-m imagery." *Continental Shelf Research*, 30: 379–392.

Poddar, S., N. Chacko, and D. Swain. 2019. "Estimation of Chlorophyll-*a* in Northern Coastal Bay of Bengal Using Landsat-8 OLI and Sentinel-2 MSI Sensors." *Front. Mar. Sci.* 6:598. doi: 10.3389/fmars.2019.00598Ruiz-Verdú, A., S. G. H. Simis, C. de Hoyos, H. J. Gons, and R. Peña-Martínez. 2008. "An evaluation of algorithms for the remote sensing of cyanobacterial biomass." *Remote Sensing of Environment*, 112(11): 3996–4008. https://doi.org/10.1016/j.rse.2007.11.019

Schalles, J., and Y. Z. Yacobi. 2000. "Remote detection and seasonal patterns of phycocyanin, carotenoid and chlorophyll-a pigments in eutrophic waters." *Archiv fur Hydrobiologie, Special Issues Advances in Limnology*, 55: 153–168

Schiebe, F. R., J. A. Harrington Jr., and J. C. Ritchie. 1992. "Remote-Sensing of Suspended Sediments—the Lake Chicot, Arkansas Project." *Int. J. Remote Sens.*, 13: 1487–1509.

Shen, L., H. Xu, and X. Guo. 2012. "Satellite remote sensing of harmful algal blooms (HABs) and a potential synthesized framework." *Sensors (Basel)*, 12(6): 7778-7803. https://doi.org/10.3390/s120607778

Simis, S. G. H., S. W. M. Peters, and H. J. Gons. 2005. "Remote sensing of the cyanobacteria pigment phycocyanin in turbid inland water." *Limn. Oceanogr.*, 50: 237–245.

Simis, S. G. H., A. Ruiz-Verdu, J. A. Domínguez-Gómez, R. Peña-Martínez, S. W. M. Peters, and H. J. Gons. 2007. "Influence of phytoplankton pigment composition on remote sensing of cyanobacterial biomass." *Remote Sens. Environ.*, 106 :414-427. https://doi.org/10.1016/j.rse.2006.09.008

Stumpf, R. P., T. W. Davis, T. T. Wynne, J. L. Graham, K. A. Loftin, T. H. Johengen, D. Gossiaux, D. Palladino, and A. Burtner. 2016. "Challenges for mapping cyanotoxin patterns from remote sensing of cyanobacteria." *Harmful Algae*, 54: 160-173. https://doi.org/10.1016/j.hal.2016.01.005

Toming, K., T. Kutser, A. Laas, M. Sepp, B. Paavel, and T. Nõges. 2016. "First Experiences in Mapping Lake Water Quality Parameters with Sentinel-2 MSI Imagery." *Remote Sensing*, 8(8):640. https://doi.org/10.3390/rs8080640

USEPA (US Environmental Protection Agency). 2012a. *Cyanobacteria and cyanotoxins: Information for drinking water systems*. Washington, DC: EPA-810F11001.

USEPA (US Environmental Protection Agency). 2012b. "The National Lakes Assessment Fact Sheet." *National Aquatic Resource Surveys*. Washington, DC.

USGS (US Geologic Survey). 2007. "The U.S. Geologic Survey Land Remote Sensing Program." Factsheet 2007-3021. https://pubs.usgs.gov/fs/2007/3021/fs2007-3021.pdf

USGS (US Geologic Survey). 2019. *Landsat 8 (L8) Data Users Handbook. Version 5.* https://prd-wret.s3.us-west-2.amazonaws.com/assets/palladium/production/atoms/files/LSDS-1574_L8_Data_Users_Handbook-v5.0.pdf

Vincent, R. K., X. Qin, R. M. L. McKay, J. Miner, K. Czajkowski, J. Savino, and T. Bridgeman. 2004. "Phycocyanin detection from LANDSAT TM data for mapping cyanobacterial blooms in Lake Erie." *Remote Sensing of Environment*, 89(3): 381-392. https://doi.org/10.1016/j.rse.2003.10.014

Wang, X., Z. Gong, and R. Pu. 2018. "Estimation of chlorophyll a content in inland turbidity waters using WorldView-2 imagery: A case study of the Guanting Reservoir, Beijing, China." *Environ Monit Assess,* 190**:** 620. https://doi.org/10.1007/s10661-018-6978-7

Wu, M., W. Zhang, X. Wang, and D. Luo. 2009. "Application of MODIS satellite data in monitoring water quality parameters of Chaohu Lake in China." *Environ Monit Assess,* 148**:** 255–264. https://doi.org/10.1007/s10661-008-0156-2

Wulder, M. A., T. R. Loveland, D. P. Roy, C. J. Crawford, J. G. Masek, C. E. Woodcock, R. G. Allen, M. C. Anderson, A. S. Belward, W. B. Cohen, J. Dwyer, A. Erb, F. Gao, P. Griffiths, D. Helder, T. Hermosilla, J. D. Hipple, P. Hostert, M. J. Hughes, J. Huntington, D. M. Johnson, R. Kennedy, A. Kilic, Z. Li, L. Lymburner, J. McCorkel, N. Pahlevan, T. A. Scambos, C. Schaaf, J. R. Schott, Y. Sheng, J. Storey, E. Vermote, J. Vogelmann, J. C. White, R. H. Wynne, and Z. Zhu. 2019. "Current status of Landsat program, science, and applications." *Remote Sens. Environ.*, 225: 127-147. 10.1016/j.rse.2019.02.015.

Wynne, T. T., R. P. Stumpf, M. C. Tomlinson, R. A. Warner, P. A. Tester, J. Dyble, and G. L. Fahnenstiel. 2008. "Relating spectral shape to cyanobacterial blooms in the Laurentian Great Lakes." *Int. J. Remote Sens.*,_ *29*: 3665–3672. https://doi.org/10.1080/01431160802007640

Yan, Y., Z. Bao, and J. Shao. 2018. "Phycocyanin concentration retrieval in inland waters: A comparative review of the remote sensing techniques and algorithms." *Journal of Great Lakes Research* 44: 748–755.

Zhao, D., X. Xing, Y. Liu, J. Yang, and L. Wang. 2010. "The relation of chlorophyll-*a* concentration with the reflectance peak near 700 nm in algae-dominated waters and sensitivity of fluorescence algorithms for detecting algal bloom." *International Journal of Remote Sensing*, 31(1): 39-48. DOI: 10.1080/01431160902882512

REPORT DOCUMENTATION PAGE

Form Approved
OMB No. 0704-0188

1. REPORT DATE ***(DD-MM-YYYY)*** June 2022	**2. REPORT TYPE** Final	**3. DATES COVERED** ***(From - To)***
4. TITLE AND SUBTITLE A Review of Empirical Algorithms for the Detection and Quantification of Harmful Algal Blooms Using Satellite-Borne Remote Sensing		**5a. CONTRACT NUMBER** **5b. GRANT NUMBER** **5c. PROGRAM ELEMENT NUMBER**
6. AUTHOR(S) Richard A. Johansen, Molly K. Reif, Christina L. Saltus, and Kaytee L. Pokrzywinski		**5d. PROJECT NUMBER** **5e. TASK NUMBER** **5f. WORK UNIT NUMBER**
7. PERFORMING ORGANIZATION NAME(S) AND ADDRESS(ES) (continued) See reverse		**8. PERFORMING ORGANIZATION REPORT NUMBER** ERDC/EL SR-22-2
9. SPONSORING / MONITORING AGENCY NAME(S) AND ADDRESS(ES) Aquatic Nuisance Species Research Program US Army Engineer Research and Development Center Environmental Laboratory Vicksburg, MS 39180-6199		**10. SPONSOR/MONITOR'S ACRONYM(S)** **11. SPONSOR/MONITOR'S REPORT NUMBER(S)**

12. DISTRIBUTION / AVAILABILITY STATEMENT
Approved for public release; distribution is unlimited.

13. SUPPLEMENTARY NOTES

Funding Account Code U4377111; AMSCO Code 096 3123 495

14. ABSTRACT

Harmful Algal Blooms (HABs) continue to be a global concern, especially since predicting bloom events including the intensity, extent, and geographic location, remain difficult. However, remote sensing platforms are useful tools for monitoring HABs across space and time. The main objective of this review was to explore the scientific literature to develop a near-comprehensive list of spectrally derived empirical algorithms for satellite imagers commonly utilized for the detection and quantification HABs and water quality indicators. This review identified the 29 WorldView-2 MSI algorithms, 25 Sentinel-2 MSI algorithms, 32 Landsat-8 OLI algorithms, 9 MODIS algorithms, and 64 MERIS/Sentinel-3 OLCI algorithms. This review also revealed most empirical-based algorithms fell into one of the following general formulas: two-band difference algorithm (2BDA), three-band difference algorithm (3BDA), normalized-difference chlorophyll index (NDCI), or the cyanobacterial index (CI). New empirical algorithm development appears to be constrained, at least in part, due to the limited number of HAB-associated spectral features detectable in currently operational imagers. However, these algorithms provide a foundation for future algorithm development as new sensors, technologies, and platforms emerge.

15. SUBJECT TERMS
Algal blooms – Monitoring
Remote sensing
Remote – sensing images
Algorithms – evaluation
Water quality management

16. SECURITY CLASSIFICATION OF:			**17. LIMITATION OF ABSTRACT**	**18. NUMBER OF PAGES**	**19a. NAME OF RESPONSIBLE PERSON**
a. REPORT	**b. ABSTRACT**	**c. THIS PAGE**			**19b. TELEPHONE NUMBER** ***(include area code)***
Unclassified	Unclassified	Unclassified	SAR	40	

Standard Form 298 (Rev. 8-98)
Prescribed by ANSI Std. 239.18

7. PERFORMING ORGANIZATION NAME(S) AND ADDRESS(ES) (concluded)

Environmental Laboratory
U.S. Army Engineer Research and Development Center
3909 Halls Ferry Road
Vicksburg, MS 39180-6199

Environmental Laboratory
U.S. Army Engineer Research and Development Center
Joint Airborne Lidar Bathymetry Technical Center of Expertise
7225 Stennis Airport Rd. Suite 100
Kiln, MS 39556

National Centers for Coastal Ocean Science
National Oceanic and Atmospheric Administration
101 Pivers Island Rd
Beaufort, NC 28516